Biogeosciences Discuss., 6, 3803–3850, 2009
www.biogeosciences-discuss.net/6/3803/2009/

Biogeosciences Discussions

Biogeosciences Discussions is the access reviewed discussion forum of *Biogeosciences*

Dissolved iron (II) in the Baltic Sea surface water and implications for cyanobacterial bloom development

E. Breitbarth[1,2,*], J. Gelting[2], J. Walve[3], L. J. Hoffmann[1,*,4], D. R. Turner[1], M. Hassellöv[1], and J. Ingri[2]

[1]Department of Chemistry, Analytical and Marine Chemistry, University of Gothenburg, Kemivägen 10, 412 96 Gothenburg, Sweden
[2]Luleå University of Technology, Division of Applied Geology, 97187 Luleå, Sweden
[3]Department of Systems Ecology, Stockholm University, 10691 Stockholm, Sweden
[4]Department of Plant and Environmental Sciences, University of Gothenburg, Box 461, 40530 Gothenburg, Sweden
[*]now at: Department of Chemistry, University of Otago, PO Box 56, Dunedin 9054, New Zealand

Received: 28 February 2009 – Accepted: 23 March 2009 – Published: 6 April 2009

Correspondence to: E. Breitbarth (ebreitbarth@chemistry.otago.ac.nz)

Published by Copernicus Publications on behalf of the European Geosciences Union.

Abstract

Iron chemistry measurements were conducted during summer 2007 at two distinct locations in the Baltic Sea (Gotland Deep and Landsort Deep) to evaluate the role of iron for cyanobacterial bloom development in these estuarine waters. Depth profiles of Fe(II) were measured by chemiluminescent flow injection analysis (CL-FIA) and reveal several origins of Fe(II) to the water column. Photoreduction of Fe(III)-complexes and deposition by rain are main sources of Fe(II) (up to 0.9 nmol L^{-1}) in light penetrated surface waters. Indication for organic Fe(II) complexation resulting in prolonged residence times in oxygenated water was observed. Surface dwelling heterocystous cyanobacteria where mainly responsible for Fe(II) consumption in comparison to other phytoplankton. The significant Fe(II) concentrations in surface waters apparently play a major role in cyanobacterial bloom development in the Baltic Sea and are a major contributor to the Fe requirements of diazotrophs. Second, Fe(II) concentrations up to 1.44 nmol L^{-1} were observed at water depths below the euphotic zone, but above the oxic anoxic interface. Finally, all Fe(III) is reduced to Fe(II) in anoxic deep water. However, only a fraction thereof is present as ferrous ions (up to 28 nmol L^{-1}) and was detected by the CL-FIA method applied. Despite their high concentrations, it is unlikely that ferrous ions originating from sub-oxic waters could be a temporary source of bioavailable iron to the euphotic zone since mixed layer depths after strong wind events are not deep enough in summer time.

1 Introduction

1.1 Iron and marine biogeochemistry

Iron and other trace metals have essential roles in the biosphere, serving as the active centers of enzymes and are responsible for electron transfer reactions in different vital biological processes. The large scale multi-disciplinary iron enrichment experi-

ments in HNLC (High Nutrient Low Chlorophyll) regions demonstrated the role of iron and co-limitation with factors such as light and macronutrients on marine biogeochemical cycles (de Baar et al., 2005; Boyd et al., 2007). Generally, iron and other trace metal control of primary production in coastal and estuarine like waters such as the Baltic Sea is not considered at first hand. However, more than 99% of the total iron concentration in seawater is organically complexed (Rue and Bruland, 1995). Thus, even if replenished at high concentrations, iron bioavailability for marine algae largely is regulated by organic complexation and observations of iron control in nutrient replete coastal waters indicate that due to strong DOM-Fe complexation, iron limitation is not confined to the classic HNLC regions (Öztürk et al., 2002a; Hutchins et al., 1998). Therefore, the paradigm of generally iron-replete and iron-deficient systems may need to be refined for some coastal areas, especially with respect to seasonal variations in iron speciation.

In seawater, iron occurs in two oxidation states, Fe(II) and Fe(III). Thermodynamics strongly favor Fe(III) in the modern oxygenated ocean, whereas its solubility is low and only maintained at sufficient concentrations for phytoplankton growth by organic complexation (Bruland et al., 2003; Rue and Bruland, 1995). In contrast, Fe(II) is highly soluble but rapidly re-oxidized to Fe(III) in oxygenated seawater (Santana-Casiano et al., 2006). Next to oxygen, hydrogen peroxide, and reactive oxygen species; seawater pH and water temperature further affect Fe(II) oxidation rates (Croot et al., 2001; Millero and Sotolongo, 1989; Millero et al., 1987). Direct photolysis of organic Fe(III) complexes in surface water can be a significant source of Fe(II) in seawater (Barbeau et al., 2003; Croot et al., 2008), while photoreduction of inorganic iron species at seawater pH is negligible (King et al., 1993). Fe(II) is considered both more labile and bioavailable than complexed Fe(III) since uptake of Fe(II) does not require energetically costly surface reduction of iron at the cell membrane, or across membrane transport of specific iron ligand complexes (Morel et al., 2008; Sunda, 2001; Anderson and Morel, 1982).

1.2 The Baltic Sea, cyanobacterial blooms, and iron

The Baltic Sea (Fig. 1) is the worlds largest estuary and forms a unique and multifaceted coastal and marine environment due to strong physico-chemical gradients, land influences (run-off water, riverine and melt-water input), and episodic oceanic water inflow. The Baltic Sea is extensively used as a waterway, fishing ground, and for recreational purposes. Thus it is of high socio-economic value to its riparian nations. The Baltic Sea ecosystem as a whole has gained more and more attention and monitoring studies and satellite observations have shown varying extents of surface slicks with massive cyanobacterial abundances over the past years (Kahru et al., 2007). The Baltic Proper, with the Gotland Basin in its center and the Landsort Deep station on its northwestern margin, is considered as the origin of cyanobacterial bloom development during summers due to favorable conditions for their growth with regard to salinity and DIN:DIP ratios seasonally as low as 1 (Stal et al., 2003).

Cyanobacterial nitrogen fixation accounts for 20–40% of the nitrogen input into the Baltic Sea (Larsson et al., 2001). Low N:P ratios favor nitrogen fixation and cyanobacterial blooms generally develop over the course of the summer after eukaryotic phytoplankton has diminished dissolved nitrogen sources. On the one hand, the increase in cyanobacteria occurrence and density has been attributed to eutrophication (Finni et al., 2001). Alternatively, phosphorus release from up-welled deep waters may stimulate cyanobacteria growth (Stal et al., 2003; Kononen et al., 1996). Iron as a potentially limiting nutrient for cyanobacterial bloom development and nitrogen fixation in the Baltic Sea has been suggested (Stal et al., 1999; Stolte et al., 2006). N_2 fixing cyanobacteria have a 2.5–11 fold higher iron demand than other phytoplankton (Kustka et al., 2003b; Kustka et al., 2002, 2003a; Sanudo-Wilhelmy et al., 2001) and thus cyanobacterial bloom development may to some extent be controlled by iron bioavailability. Coastal waters can have a high load of dissolved organic matter (DOM) and photoreduction of Fe bound to DOM and specifically also phytoplankton exudates after previous spring blooms can yield higher Fe(II) concentrations than in open ocean water. Further, ver-

tical mixing can introduce high loads of Fe(II) from anoxic sediments into coastal surface water (Kuma et al., 1992, 1995). Since Fe(II) is unspecifically available to all phytoplankton its presence may imply favorable growth conditions and an ecological advantage for surface dwelling nitrogen fixing cyanobacteria over other phytoplankton if concentrations of other inorganic nitrogen sources are low.

The distributions of trace metals along the north-south salinity gradient in surface waters of the Baltic Sea and in depth profiles across the redox-cline that divide the water column in an oxygenated and phosphate depleted surface zone and an anoxic, metal and phosphate rich deep water layer have been addressed (Brügmann et al., 1992). Brügmann et al. (1998) and Pohl and Hennings (1999) have described metal speciation changes after the 1993/94 salt water inflow and resulting bottom water oxygenation events. However, deep water anoxic conditions reestablished and no salt water inflow event was precluding our field season in the summer of 2007. Further, Ingri et al. (2004) showed a shift in trace metal speciation from the low molecular weight (LMW) fraction into the colloidal and particulate phase over the course of a spring bloom, which would result in seasonal depletion of potentially bioavailable LMW bound trace metals. The Landsort Deep and Gotland Deep regions of the Baltic Sea are characterized by surface dissolved Fe concentrations in the low nanomolar range (Strady et al., 2008; Gelting et al., 2009b). Yet, to date no specific data on iron complexation and surface or deep water concentrations of Fe(II) in Baltic Sea waters exist.

1.3 Aim of the study

In this study, we address the dynamics of Fe(II) concentrations over the course of the Nordic summer covering the full depth range at these two locations. The approach takes the main source for Fe(II) photoreduction in surface water (organically complexed iron), next to physico-chemical parameters (irradiation, temperature) and main oxidants (oxygen, hydrogen peroxide), as well as indicators for consumption (chlorophyll-*a*, cyanobacteria biomass) into account. Depth profiles also aim to indentify other sources of Fe(II) and set them in context of interactions with additional parameters

(pH, total phosphate (PO_4), total hydrogen sulfide (H_2S)) and water column mixing.

We hypothesize that iron has a regulatory function during cyanobacterial bloom development in the Baltic Sea and particularly that Fe(II) concentrations may play an important role. We evaluate if A: Fe(II) and PO_4 rich water masses from deeper oxygen depleted layers can be mixed into surface waters after storm events and; and B: if photoreduction from Fe(III) organic complexes is a significant source of Fe(II) to the euphotic zone (Fig. 2). To the best of our knowledge, this is the first comprehensive study focusing on Fe(II) throughout the water column in estuarine water. While the study aims to contribute to the general understanding of marine Fe redox cycling and biological processing, it is of additional relevance for other estuarine and coastal waters, as well as oceanic regions with oxygen minimum zones or sub-oxic bottom water.

2 Methods

2.1 Cruise locations

A total of five cruises were conducted using the R/V *Fyrbyggaren* between 20 June and 14 August 2007 to two stations in the Baltic Sea. Landsort Deep (459 m depth, 58°36′ N, 18°14′ E) is located close to the Swedish east coast and Gotland Deep (249 m depth, 57°18′ N; 20°04′ E) is situated in the center of the main basin of the Baltic Proper (Fig. 1). Both stations are characterized by a clear redox-cline at intermediate depth. Fresher estuarine Baltic water on the surface overlays more saline water at depth. The deep water is anoxic after extended periods of time of limited exchange with the upper layer. It typically is rich in macro nutrients, especially PO_4, and metal concentrations and characterized by hydrogen sulfide formation after microbial oxygen consumption. However, influx events of oxic marine water from the Skagerrak through the Danish Straits can perturb and oxygenate the deep water layer, as for example recorded for 1993/94, 1997, and 2003/04 (Meier, 2007). Such influx and oxygenation events can largely alter the nutrient and metal chemistries and result in precipitation of metal salts.

BGD
6, 3803–3850, 2009

This, however, was not the case during our study.

2.2 Seawater sampling and sample processing

Surface water samples (5 m depth) were obtained using trace metal cleaned polyethylene (PE) tubing that was suspended by a 16 m plastic mast from the bow of the vessel. The vessel steamed at speed of 1 kn into the wind during surface sampling to minimize the risk of contamination by the ship. The sampled water was transported via a peristaltic pump into a laminar flow bench inside a laboratory container, where all sample handling took place. Water for measurements of dissolved iron, iron ligand titrations, and deck incubations was filtered through trace metal cleaned 0.2 μm polycarbonate membranes. Depth profiles were sampled using individual pre-washed all plastic Niskin bottles with elastic silicone bands as the closure mechanism.

Samples for Fe(II) and hydrogen peroxide (H_2O_2) analysis were drawn from the Niskin bottles immediately after retrieval on deck into a 50 ml PE syringe. Subsequently, the water was passed through a pre-washed 0.45-μm-pore size PVDF membrane (Sterivex-HV®, Millipore) and split into two PE vessels. Fe(II) concentrations were determined within the shortest time possible, usually within four minutes after sampling for oxygenated surface water (the exact timing from sampling to analysis was noted) and a maximum of one hour after sampling for anoxic deep water. Samples for dissolved oxygen were taken immediately after the Fe(II)/H_2O_2 samples. H_2O_2 samples were stored in the dark for a minimum of two hours prior to analysis. Fe(II) profiles were obtained on 4 July and 1 August, 2007, at Landsort Deep station and on 20 June, 20 July, 2 and 14 August, 2007, at Gotland Deep. H_2O_2 profiles were measured 1 August, as well as on 20 July and 2 August, 2007, at Landsort Deep and Gotland Deep, respectively.

2.3 Fe(II) analysis

Seawater was analyzed for its Fe(II) content based on Croot and Laan (2002) using Chemiluminescent Flow Injection Analysis (CL-FIA) with a luminol (5-amino-2,3-dihydro-1,4-phthalazine-dione) reagent. The flow injection analyzer (FIA, Waterville Analytical, Maine, USA) was equipped with a 50 cm (1.2 mL) sample loop. No sample pre-concentration steps were applied. The effluent pH was monitored and adjusted to 10.3–10.4. A custom made Labview (National Instruments, USA) based software was used for instrument control and data acquisition. The measurements were calibrated using standard additions. A 10 mM primary Fe(II) standard solution was prepared from a Merck Titrisol Fe(II) standard in 0.1 M HCL. Secondary standards were prepared immediately prior to use by serial dilution of the primary standard using 0.01 M HCl. Standard additions to the samples were kept below 0.1% volume to reduce the effect of lowering the sample pH to a minimum. Oxidation rates were calculated based on Millero et al. (1987) after approximating $[OH]^-$ using the the program CO_2SYS (Lewis and Wallace, 1998). (see also Sect. 2.9).

2.4 Hydrogen peroxide analysis

H_2O_2 concentrations were determined by CL-FIA based on Yuan and Shiller (1999) using a second flow injection analyzer similar to the one described above. A 60 μL reagent loop was used. The analysis utilizes the oxidation of luminol by H_2O_2 in an alkaline solution, which is catalyzed by cobalt(II). Standards for standard addition calibrations were made using 30% H_2O_2 obtained from Fluka (trace select). Signal values from depths with no presence of H_2O_2 were reproducibly lower than blanks from using aged MQ water (indicating presence H_2O_2 in the MQ water), and thus subtracted as blank values. Samples were only measured to the depth of the redox-cline since high Fe(II) concentrations interfere with the analysis (Yuan and Shiller, 1999).

2.5 Deck incubations

At GD (20 July) seawater incubations were performed in a series of 24 trace metal clean quartz glass bottles (30 ml). Seawater was collected as described above on the evening prior to the experiment and the bottles were completely filled, without any visible air bubbles and stored in the dark overnight. The storage temperature equaled the ambient seawater temperature. The incubation was started at 06:00 the following morning in two deck mounted incubators at ambient seawater temperature using surface seawater supplied from the ships fire hose for temperature control. Natural sunlight was shielded to 50% light intensity using neutral density screening. The water was subjected to four treatments: unfiltered, 0.2 μm filtered (see section above), 10 μm filtered through a trace metal cleaned Nitex mesh (to remove cyanobacterial aggregates, but retain other phytoplankton), and enriched with cyanobacteria (pre-collected on a 10 μm trace metal cleaned Nitex mesh). At three time points (10:00, 13:30, and 16:40) discrete bottles were analyzed for their Fe(II) and H_2O_2 concentrations as described above.

2.6 Organic iron(III) complexation

Filtered seawater samples (0.2 μm) from the GD samplings were analyzed for organic iron complexation using competitive ligand exchange cathodic stripping voltammetry (CLE-CSV). A Metrohm VA 993 Computrace equipped with a hanging mercury drop electrode, glassy carbon counter electrode, and Ag/AgCl reference electrode was used. In general, iron was titrated by standard additions against a 0.01 M solution of 2-(2-Thiazolylazo)-p-cresol (TAC) competing with the natural ligands for iron complexation in a EPPS buffered (pH: 8.0) seawater sample based on Croot and Johansson (2000). All analyses were performed on frozen and re-thawed seawater samples at 20°C in a 10 step titration series. Iron binding ligand concentrations and their conditional stability constants with respect to Fe' (log $K_{Fe'L}$, inorganic side reaction coefficient $\alpha_{Fe'}=10^{10}$) were calculated from the titration curves using a single ligand model

and applying a nonlinear fit to a Langmuir absorption isotherm (Croot and Johansson, 2000; Gerringa et al., 1995). Dissolved iron concentrations (ICP-MS measurements) are obtained from size fractionated iron analyses conducted in a parallel study (Gelting et al., 2009a).

2.7 DGT methodology

Diffusive gradients in thin films (DGT) equipped with open pore (APA2) gels were used to sample the labile fraction of Fe (Davison and Zhang, 1994). Preparation of the gels followed procedures described earlier (Dahlqvist et al., 2002; Zhang and Davison, 1999). The labile Fe concentrations were calculated from the accumulated amounts in the DGTs according to Zhang and Davison (1995). The diffusion coefficient for Fe (received from DGT Research Ltd) was corrected for average temperatures measured in situ every five during the deployment period. All DGT units were assembled in a clean air trace metal laboratory and stored in clean plastic bags at 4°C before use. Blanks (not deployed in water) from each batch of assembled DGTs were measured and subtracted from the calculated labile Fe concentrations derived from the deployed DGTs. Labile concentrations are reported as the average result from duplicates. DGTs were deployed at 2 occasions, 24 May and 20 July 20, for 4 weeks. DGT units were deployed at 0.5, 5, 10, 40, and 120 m depth in a buoy system described by Forsberg et al. (2006). After collection, the DGT units were rinsed in MilliQ water, placed in clean, airtight plastic bags and stored at 4°C until analysis. The DGT devices were disassembled again in a clean air trace metal laboratory and the gels were eluted in 5 ml of 5 M HNO_3 (quartz-distilled). Concentrations of Fe in DGT eluents and water samples were measured with an ICP-SFMS at Analytica AB in Luleå (Element, Thermo Fischer). For details about the instrument operation, see Rodushkin and Ruth (1997). Prior to analysis, water samples were diluted 4-fold with 0.16 M HNO_3 (Merck suprapur) in MilliQ water.

2.8 Reagents

Hydrochloric acid (HCL, 30%, Merck suprapur), Ammonia solution (NH_4OH, 25%, Fluka trace select), Luminol (5-amino-2,3-dihydro-1,4-phthalazine-dione), and sodium carbonate (Na_2CO_3, SigmaUltra) were used as received. A 16.97 mmol L-1 Co(II) standard solution ($CoCl_2$, Titrisol, Merck) was used to spike the luminol reagent in the H_2O_2 method to 60 μmol L^{-1}. For iron ligand titrations a 1.79 μmol L^{-1} iron standard solution in 0.01 M quartz distilled HNO_3 was prepared from a 1000 mg L^{-1} stock (Titrisol, Merck) and a 0.01 M solution of 2-(2-Thiazolylazo)-p-cresol (TAC, 97%, Sigma Aldrich) was prepared in HPLC grade methanol. EPPS buffer (N-[2-hydroxyethyl]piperazine-N'-[3-propanesulfonic acid], Sigma Ultra) was prepared in 1.0 M NH_4OH (NH_4OH, 25%, Fluka trace select) to a concentration of 1.0 M. Purified water (MilliQ, MQ) was used for all reagent preparations.

2.9 Analysis of associated parameters

Seawater pH was determined using a temperature corrected pH electrode (Metrohm, 704 pH meter), which was calibrated on the NBS/NIST scale against buffer solutions (pH 6 and 11, Merck CertiPUR) prior to each use. Second, the data were corrected to approximate the seawater pH scale using the CO_2SYS program (Lewis and Wallace, 1998), taking alkalinity and in situ temperature into account. We estimate the accuracy of this approach to be 0.05 pH units. Salinity and temperature profiles were obtained from standard CTD casts (Landsort Deep: SST Memory probe by Sea & Sun Technology GmbH, Gotland Deep: Standard-Eco-Probe by Meerestechnik GmbH and ADM Standard Probe by ADM-Elektronik GmbH), while alkalinity values are based on an alkalinity-salinity relationship for the Baltic Proper (S. Hjalmasson, personal communication, 2008). Macro-nutrients (total phosphate, NO_3 and NO_2 analyzed together, and NH_4), as well as total hydrogen sulfide, oxygen and chlorophyll-*a* (chl-a) were acquired from discrete samples, which at Landsort Deep were part of a water quality monitoring program. Samples for nutrients were filtered (0.45 μm Sarstedt Filtropur

S membrane filter) into 12 mL plastic vials, and kept refrigerated until analysed within 24 h of sampling. Samples from the deep water were heat-treated (60°C) for 1 h to kill remaining bacteria and prevent nitrification of ammonium. PO_4^{3-}, NH_4^+ and NO_2^-+NO_3^- were determined by standard methods applied in segmented flow analysis (SFA, modified ALPKEM O. I. Analytical Flow Solution IV methods # 319528, # 319526, # 319527, reporting limits: PO_4^{3-} 16 nmol L^{-1}, NH_4^+ 36 nmol L^{-1}, and NO_2^-+NO_3^- 14 nmol L^{-1}). Oxygen was determined by the Winkler method (SS-EN 25 813) and H_2S according to Fonselius et al. (1999). Where no H_2S measurements were done, the presence of H_2S smell during tapping from the Niskin bottles was recorded when present. For chlorophyll *a* determinations, 2 L of sea water were filtered on 47 mm Whatman GF/F filters, which were stored frozen and extracted by acetone before spectrophotometric measurements at 664 nmol L^{-1} (SS 02 81 46).

2.10 Cyanobacterial counts

On each occasion, three integrated phytoplankton samples (0–20 m) were collected with a 25 m long plastic tube (inner diameter 2.5 cm). One end, equipped with a weight, was gently lowered to 20 m depth, after which the tube was closed at the upper end, retrieved, and emptied in a bucket. A 200 mL sub-sample, siphoned from the bucket while stirring, was preserved with 0.8 mL of Lugol's iodine (I_2KI) solution supplemented with acetic acid. Filaments of heterocystous cyanobacteria were counted in units of 100 μm in the whole bottom of a 25 mL settling chamber using a Leica inverted phase contrast microscope (10X objective and 150X total magnification). Cell volume was estimated by multiplying the counted units with species-specific mean cell volumes, determined from measurements. To convert to carbon, factors of 2.17, 14.4 and 2.11 μg C m^{-1} filament were used for *Aphanizomenon* sp., *Nodularia spumigena* and *Anabaena* spp., respectively (Menden-Deuer and Lessard, 2000).

2.11 Meteorology

Meteorological data were obtained from the Swedish Meteorological and Hydrological Institute (SMHI) for the period 10 June–15 August 2007. Since no such data were available directly from the sampling stations, we utilized wind (speed and direction), precipitation, and global irradiation data from several locations in the closest possible vicinity (Hoburg and Visby on the island of Gotland; Östergarnsholm, a small island east of Gotland; Gotska Sandön, a small island north of Gotland; as well as Landsort A and Norrköping, which are on the Swedish mainland). Landsort A (58°75′ N, 17°87′ E) lays within relatively close proximity of the Landsort Deep station (58°36′ N, 18°14′ E), and data from there are thus representative of the weather at Landsort Deep. In contrast, the other weather observatories used for Gotland Deep are more distanced and located on or near the island of Gotland (Gotska Sandön and Östergarnsholm being closest) and the data from there are interpreted as being indicative for the conditions at this sampling station.

3 Results

3.1 General water column patterns

Surface temperatures increased from 15.4 to 19.7°C over the course of the summer at Gotland Deep (GD) and were 14.5 and 15.2°C during the two samplings at Landsort Deep (LD). Both locations, LD and GD, are characterized by a ~60 m deep layer of low salinity (S<7.5) surface water and an intermediate boundary water layer (S=7.5–11, 60–100 m) overlaying more saline deep water (S~11 at LD, S>12 at GD). A differentiation between oxygenated surface water and oxygen-depleted deeper water, separated by a redox-cline at ~80 m, was present throughout the most of the sampling period (Figs. 3a–d, 4a–d, 5a–d). A deeper, less abrupt, redox-transition zone down to 100 m was observed at GD during 14 August (Fig. 5d). Accordingly, seawater pH decreased

BGD
6, 3803–3850, 2009

by more than one unit from 8.2 to 7.0 and from 8.4–8.7 to 6.9–7.3 (also varying over time) over this depth range, at LD (Fig. 3a, b) and GD, respectively (Figs. 4a, b, 5a, b). Salinity and temperature indicate a mixed layer depth of 7 to 16 m at LD (Fig. 3a, b) and 16 to 21 m at GD (Fig. 4a, b, and Fig. 5a, b). Temperature data from 20 June at GD also indicate gradual re-stratification down to 10.5 m after previous mixing to 16 m depth (Fig. 4a). In contrast, the 20 July and 2 August casts revealed recent mixing to 11.5 m and 21 m, respectively (Figs. 4b, 5a). A second mixing event to 9.5 m depth as evident in the cast from 14 August (Fig. 5b) followed a deeper mixing to 21 m detected on 2 August (Fig. 5a).

The temperature, salinity, and PO_4 profiles of 4 July at LD show distinct perturbations of the water column between 40 and 60 m depth (Fig. 3a, c), which indicate lateral mixing of a different water mass with lower temperature and salinity. Further, lateral transport of a water mass with higher temperature was observed at 40–50 m depth at Gotland Deep on 20 July. This water mass also affected the pH profile at 40 m depth. The temperature signal persisted through 2 August, but was only reminiscent on 14 August (Figs. 4b, 5a, b).

3.2 General meteorology

The sampling period was characterized by very inconsistent weather. Periods of relatively strong winds (up to 15 m s^{-1}) from changing directions, partly associated with heavy rain, frequently altered with calmer and sunnier conditions. Of particular interest with regard to water column mixing, H_2O_2 and Fe(II) production, and rainwater input is the week directly before the sampling events. At LD, wind speeds during the 4 July sampling were exceeding 10 m s^{-1} from east and south-east, enabling a long fetch across the Baltic Sea. Significant rain deposition was also recorded prior to this sampling. In contrast, considerably weaker winds (5–8 m s^{-1}) coming with less fetch from westerly directions were persisting before and during the second sampling (1 August) at this station and thus resulted in shallower mixing. Except for the 14 August sampling at Gotland Deep, all cruises were preceded with several days of wind speeds greater

$10\,m\,s^{-1}$, mostly from westerly direction. The Gotland Deep station is located in the middle of the Baltic Proper and thus enables a relatively long wind fetch for this enclosed sea. However, none of the wind driven mixing was deep enough to disturb the water column to the oxic-anoxic transition zone.

3.3 Fe(II)

3.3.1 Fe(II) in the oxygenated water layer

At both stations, Fe(II) concentrations differ greatly between the surface and the deeper water layers below the redox-cline. Surface values measured at LD range from 0–$0.45\,nmol\,L^{-1}$, while at GD Fe(II) concentrations varied between 0 and $0.90\,nmol\,L^{-1}$. On most occasions, Fe(II) concentrations are elevated in the upper meters of the water column and decrease proportionally with depth (LD 1 August, GD 20 June, 2 and 14 August; Figs. 3f, 4f, 5e, f). At 5 m depth, chl-a increases from 1.6 to $4.1\,\mu g\,L^{-1}$ over the course of the summer and Fe(II) shows a maximum of $0.64\,nmol\,L^{-1}$ on 2 August (Fig. 6a).

Oxidation rate calculations not taking any organic Fe(II) complexation into account reveal short half life times ($t_{1/2}\,min^{-1}$) of Fe(II), which are mainly attributed to the relatively high pH in these estuarine waters. At GD at 5 m depth, $t_{1/2}$=0.32, 0.15, 0.28, and $0.04\,min^{-1}$ on 20 June, 20 July, 2 August, and 15 August, respectively. Oxidation rates were slower at LD resulting in $t_{1/2}$=1.03 and $1.00\,min^{-1}$ in surface water on 4 July and 1 August. Half-lives based on oxidation by H_2O_2 are longer throughout the data set so that only oxidation by O_2 is considered.

The LD profile on 4 July was recorded at mid-night and reveal Fe(II) persistence into the night. The sampling was preceded with 3.8 mm rain input on 3 July and 0.2 mm on 4 July. Before that, 18.9, 4.4, 0.1, and 2.3 mm precipitation was recorded on 26, 27, 28, and 30 June, respectively. However, the detected 0.45 and $0.43\,nmol\,L^{-1}$ Fe(II) at 40 and 60 m, respectively (Fig. 3e), are below the mixing depth and thus are unlikely

a product of recent rain deposition. This Fe(II) peak is paralleled by a temperature, salinity, and PO_4 signal, which indicate lateral transport of a different water mass. This signal was only reminiscent on 1 August.

Highest values were not always measured in the upper, most light pervaded, meters of the oxygenated water column. Elevated Fe(II) levels were also detected at several tenths of meters water depth, but clearly above the redox-cline, during nearly all cruises. Most prominently, this was the case on 4 July at LD (see above), but also at 2 August at GD (0.85 nmol L^{-1} at 40 m and 1.44 nmol L^{-1} at 80 m, Fig. 5e) and 14 August at GD (0.15 nmol L^{-1} at 60 m, Fig. 5f). Secchi depths ranged from 4.5–5.5 m throughout the samplings at both stations and thus also indicate insufficient light penetration for photochemical production of Fe(II) to these depths. However, in almost all cruises Fe(II) levels drop to zero at some point in the profile. A different pattern was only observed on 20 June at GD, where Fe(II) levels progressively increased with depth from 40 m on already (Fig. 4e). Further, at both stations O_2 was present at these depths, albeit already at low levels. O_2 concentrations within this depth range indicate the transition from oxygenated surface water towards the oxic-anoxic interface (Figs. 4c, d, 5c, d).

3.3.2 Deep water Fe(II)

In contrast to oxygenated surface water, measurements of Fe(II) in anoxic deep water at the two stations in the Baltic reveal a relatively constant pattern. At LD, concentrations rapidly exceed 10 nmol L^{-1} below the redox-cline, show at maximum of 21.4–23.4 nmol L^{-1} at 100–150 m depth, which parallels maximum H_2S values and decline again to 14.6–16.6 nmol L^{-1} in near bottom waters (Fig. 3c–f). Following a similar pattern at GD, Fe(II) reaches a maximum of 21.5–28.6 nmol L^{-1} at 170 m, except on 20 July where only 15.6 nmol L^{-1} were detected. Bottom water values generally were several nanomoles lower. However, on 2 August the maximum (26.6 nmol L^{-1}) was measured at 200 m depth (Figs. 4e, f, 5e, f). This coincided with a deepening of the onset of the H_2S signal in the water column from 140 m to 170 m and a PO_4 peak of 5.4 μmol $^{-1}$

at 140 m (Figs. 4c, d, 5c, d), as well as >0.1 units lower pH values (7.07–7.10) below the redox-cline (Figs. 4a, b, 5a, b).

3.4 Hydrogen peroxide (H_2O_2)

H_2O_2 profiles were measured on 1 August at LD, where maximum concentrations of 14.2 nmol L^{-1} at 0.5 m depth are generally up to an order of magnitude lower than concentrations at GD. A subsurface peak of 12.6 nmol L^{-1} was detected at 20 m depth and values decrease to 0 at 70 m depth. The measurement 0.35 nmol L^{-1} H_2O_2 in the suboxic water (0.43 mg L^{-1}) at 80 m depth may be interfered by high Fe(II) concentrations (7.25 nmol L^{-1}, Fig. 3f). At GD, two sampling occasions (20 July and 2 August) included H_2O_2 measurements and revealed differing results. Like at LD, H_2O_2 levels on 2 August at GD decreased with depth as an apparent function of light penetration into the water column from 68.4 nmol L^{-1} at the surface to 4.5 nmol L^{-1} at 80 m depth. The 182 nmol L^{-1} H_2O_2 measured at 100 m depth may be erroneous, since no other parameter shows such a peak at this depth and an interference in the chemiluminescent measurement with Fe(II) is unlikely due to its still low concentration (0.71 nmol L^{-1}). No H_2O_2 was detected at 120 m depth (Fig. 5e). In contrast to this profile, H_2O_2 measurements from the same station at the earlier 20 July sampling are considerably higher. In the upper 10 m of the water column values greater 130 nmol L^{-1} were measured and a peak of 160 nmol L^{-1} was detected a 5 m. However, below 10 m the H_2O_2 increases again and peaks at 40 m depth (231 nmol L^{-1}). Thereafter, values decrease gradually to 0.34 nmol L^{-1} at 120 m depth (Fig. 4f).

3.5 Phytoplankton biomass

Chlorophyll–*a* (5 m depth) increased over the summer from 1.2 μg L^{-1} to 4.1 μg L^{-1}, with a strong gain between 2 and 14 August (Fig. 6a). The biomass of heterocystous cyanobacteria was initially dominated by *Aphanizomenon* sp. (Fig. 6b). This genus peaked on 20 June (15 μg C L^{-1}) and thereafter its biomass progressively decreased

again. In parallel, a decrease from 3.5 to 1 heterocyst per mm filament was observed in this genus (data not shown). The two other cyanobacteria genera that majorly accounted for the biomass were *Nodularia* and *Anabena*. *Anabaena* showed a similar development in biomass as *Aphanizomenon*, albeit peaking at much lower concentrations ($1.6\,\mu g\,C\,L^{-1}$). The *Nodularia* biomass reached its maximum 20 July ($17\,\mu g\,C\,L^{-1}$) and thereafter dropped by more than 50% (2 August) and slightly recovered to $11\,\mu g\,C\,L^{-1}$ on 14 August. The combined biomass of all three genera though was elevated during 20 June–20 July ($25–28\,\mu g\,C\,L^{-1}$, Fig. 6b). The cyanobacterial biomass is integrated over the top 20 m. Concentrations at 5 m depth may well be higher, especially when the mixed layer is shallow and particularly for *Nodularia*, which has high a buoyancy and usually accumulates in the surface (Walve and Larsson, 2007).

3.6 Total and dissolved iron concentrations and organic iron(III) complexation at 5 m depth

At GD, total iron concentrations increase from 10.6 nmol L^{-1} on 24 May to 12.9 nmol L^{-1} on 20 June. Levels are lowest in mid-June (7.5 nmol L^{-1}) and increase again to 11.7 nmol L^{-1} on 14 August. Dissolved iron concentrations follow this trend during the first part of the summer with 2.8 nmol L^{-1} on 24 May and 7.0 nmol L^{-1} on 20 June. However, thereafter levels gradually decrease to 2.7 nmol L^{-1} on 14 August. Thus the source of total iron input in the end of the summer does not affect dissolved iron concentrations to the same extent as observed during the 20 June sampling (Fig. 7a). Iron binding ligands decline gradually from 11.5 to 2.7 nmol L^{-1} between 24 May and 2 August causing the surface seawater to be deficient of organic iron ligands from 20 June on. Ligand concentrations in excess of dissolved iron concentrations were only detected again on the last cruise on 14 August (3.0 nmol L^{-1}, Fig. 7b). Overall, the source of iron binding ligands is apparently decoupled from the source of total iron input. The conditional stability constant (log $K_{Fe'L}$) increased from 10.33 to 11.75 from 24 May to 20 June and slightly decreases thereafter with a clear drop from 11.55 to 11.19 between 2 and 14 August. The concentrations of Fe' range from 5 to 9 pmol L^{-1}

and peak on 20 June. The trend in Fe' anti-correlates the excess ligand concentrations (Fig. 7b).

3.7 DGT data

DGT profiles resemble Fe(II) measurements in the oxygenated part of the water column. At the sea surface, DGT collected iron is elevated (0.63 and 0.42 nmol L^{-1} during the periods 24 May–20 June and 20 July–14 August, respectively). In both profiles, the signal decreases to 0.17–0.28 nmol L^{-1} at 5–10 m depth. In the first sampling interval, DGT measured iron progressively increases thereafter to 0.96 nmol L^{-1} at 80 m and then decreases to 0.74 nmol L^{-1} at 120 m depth. In contrast, the signal remains more constant to 40 m depth (0.22 nmol L^{-1}), and increases to 1.57 nmol L^{-1} (closely matching 1.44 nmol L^{-1} in the Fe(II) profile from 2 August) at 80 m depth during the second time period. The signal though clearly exceeds any FIA measured Fe(II) concentrations during this study with 63.4 nmol L^{-1} at 120 m depth (Fig. 8a, b).

3.8 Macronutrients at 5 m depth

At GD, PO_4 concentrations decrease from 179 to 12 nmol L^{-1} between 24 May and 2 August and slightly recover to 24 nmol L^{-1} on 14 August (Fig. 9a). The highest dFe to PO_4 ratio (0.26, molar basis) was observed on 2 August (Fig. 9b). Combined NO_3+NO_2 analysis showed concentrations close to the detection limit on all occasions. Also NH_4 concentrations were low (<80 nmol L^{-1}) (Fig. 9a). Comparing combined dissolved inorganic nitrogen sources (DIN=NO_3+NO_2+NH_4) with dissolved iron concentrations reveal a maximum dFe:DIN molar ratio of 0.082 on 20 June (Fig. 9). DIN:DIP ratios at Gotland Deep were 0.5 on 25 May. As PO_4 dropped, the ratio increased to 2.3, and 3.3 on 20 June and 20 July, respectively, and further increased to 7.4 by 2 August, after which the ratio dropped again to 2.8. At the Landsort Deep, DIN:DIP stoichiometry was 7.4 and 6.0 during 4 July and 2 August, respectively.

3.9 Deck incubation experiment – H_2O_2 and Fe(II) production and consumption

Cyanobacterial counts show that *Aphanizomenon* and *Nodularia*, but no *Anabaena* were present in the incubations. The up-concentration factor was ~70 fold. H_2O_2 concentrations continuously increase over the course of the day (Fig. 11a). No clear difference was detected in H_2O_2 values of the fractions that were depleted or enriched in cyanobacteria, or remained unchanged. The 0.2 μm filtered seawater however increased from 699 to 3229 nmol L^{-1} during the day (Fig. 11a) and is thus considerably higher than levels detected in the depth profile at this station on the same day (Fig. 4f). Fe(II) concentrations show a peak during midday (except for the treatment that was depleted in cyanobacteria) and differ among all treatments. The 0.2 μm filtered seawater (peaking at 1.28 nmol L^{-1}) also exceeds levels measured at 5 m depth in the profile (0.267 nmol L^{-1}, Fig. 4f). However, values approaching 1 nmol L^{-1} have been detected directly at the sea surface on 2 August (Fig. 5e). Considering the short half life time of Fe(II) in oxygenated seawater and the time offset between measurements of the incubation and the profile, this difference may in part be due to changing solar irradiation. Most pronounced are differences to the incubations that were enriched with cyanobacteria, which are one order of magnitude lower in Fe(II) concentrations. Further, the incubations depleted in heterocystous cyanobacteria accumulate Fe(II) over the course of the day from 0.378 to 0.962 nmol L^{-1}. Unaltered seawater showed the highest Fe(II) levels in the morning (0.926 nmol L^{-1}), but thereafter follows the same trend as 0.2 μm filtered seawater.

4 Discussion

4.1 Main findings

Overall this study aims to contribute to the understanding of iron cycling in the Baltic Sea. Specifically, it was the goal of our approach to evaluate the role of Fe and espe-

cially of Fe(II) for cyanobacterial bloom development in this brackish water ecosystem. We identified three distinct sections in the water column, which each show individual characteristics of Fe(II) cycling. A – The fully oxygenated euphotic zone where photoreduction of Fe(III)-complexes and deposition by rain are the main sources of Fe(II). B – Lateral transport of water masses can introduce Fe(II) into the oxic-anoxic transition zone above the pycnocline. And second, local production by iron reducing bacteria may elevate Fe(II) concentrations in this sub-oxic part of the water column. C – The deep and bottom waters of the Gotland Basin and the Landsort Deep are an anoxic and reducing regime, resulting in reduction of all Fe(III) to Fe(II) and finally the formation of iron sulfide.

4.2 Fe(II) in the oxic-anoxic transition zone and in anoxic deep water

We hereafter mainly focus on the oxygenated surface water layer. Detailed results from the anoxic deep water and oxic anoxic transition zone will be published elsewhere. Just in brief, Fe(II) concentrations below the redox-cline range between 10–25 nmol L^{-1} at Landsort Deep (Fig. 3e, f) and comparable 8–27 nmol L^{-1} at Gotland Deep (Figs. 4 e, f, 5e, f). Thermodynamics favor all iron in this water layer to be reduced to Fe(II) as also suggested by Strady et al. (2008). The Luminol chemiluminescent flow injection analysis (CL-FIA) used for the Fe(II) measurements here (Croot and Laan, 2002; Rose and Waite, 2001) apparently only detects the ferrous ions and is insensitive to iron sulfides, explaining the discrepancy between Fe(II) and total dissolved Fe measurements in anoxic deep water at the Gotland Deep station, which differ by one order of magnitude considering the total dissolved Fe data provided by Strady et al. (2008). Fe(II) levels detected in anoxic waters at Landsort Deep, correlate with H_2S data (Fig. 3c–f), indicating the formation process of ferrous ions and hydrogen sulfides to iron sulfides and further supporting the specificity of Luminol CL-FIA to ferrous ions. Thus this method alone is not fully suitable to determine the total concentrations of iron in the 2^+ oxidation state in anoxic water. However, Luminol CL-FIA provides a highly sensitive tool to measure Fe(II) ions and is thus excellently suited for studying sub-oxic

and oxygenated waters, where no sulfides are present (Croot and Laan, 2002; Rose and Waite, 2001). The prominent Fe(II) concentrations in the intermediate water layer (oxic-anoxic transition zone and above) at both stations are below the 1% light level (~10 m depth) and thus too deep for photoreduction or rain deposition as production pathways. Further, any wind driven mixing of the water column during the study period was not deep enough to reach the oxic-anoxic transition zone. The maximum mixing depth observed was 21 m at Gotland Deep as observed on 2 August 2008 (Fig. 5a). Thus either a local source, such as microbial iron reduction in sub-oxic waters as suggested by Moffett et al. (2007) or isopycnal transport of water that previously passed over reducing sediments before entering the Gotland Basin may be responsible for the Fe(II) signal within this depth range. Any Fe(II) present in surface water must be locally produced and a resupply together with PO_4 from deep water is very unlikely during summer time.

4.3 Fe(II) in the oxygenated water layer

In the oxygenated and euphotic upper water layer, Fe(II) is largely produced photochemically (Kuma et al., 1995; Wells and Mayer, 1991; Croot et al., 2001), but can also be deposited during rain events (Kieber et al., 2001), a product of biological Fe(III) reduction at phytoplankton cell surfaces (Shaked et al., 2004) or after extracellular superoxide production (Kustka et al., 2005). However, it is not known if heterocystous cyanobacteria reduce Fe(III) at their cell surfaces. Our data imply that especially wet deposition and photochemical reduction of organic Fe(III)-complexes are important sources of Fe(II) to the surface layer at Gotland Deep and Landsort Deep.

4.3.1 The role of organic Fe(III) complexation

While organically complexed dissolved iron is progressively decreasing at Gotland Deep over the course of the study (Fig. 7b), this substratum for photoreduction of iron apparently is present at sufficient levels since Fe(II) concentrations do not correlate with

iron ligand concentrations. The decrease of iron binding ligands parallels the decrease in PO_4 and anti-correlates with chlorophyll–*a* increase at 5 m water depth (Figs. 6a, 9a). Therefore, biological uptake of ligand bound iron probably is responsible for this trend in parallel to dissimilatory photoreduction of dissolved organic matter. Moreover, the conditional stability constant of iron binding ligands in the beginning of the study (log $K_{Fe'L}$=10.3, Fig. 7b) closely resembles that reported for fulvic acid isolated from river natural organic matter (log $K_{Fe'L}$=10.4, Rose and Waite, 2003). During the middle of the summer log $K_{Fe'L}$ is elevated (>11.5) and approaches the strength of marine iron binding ligands (Rue and Bruland, 1995; Witter et al., 2000), but decreases again between the 2 and 14 August sampling (Fig. 7b). At the same time chlorophyll–*a* and iron ligand concentrations increase again. This indicates that the iron ligand characteristics are connected to the phytoplankton bloom dynamics and that at least a proportion of the ligands present may be biologically produced. Further, the chlorophyll–*a* and *Nodularia* biomass increase in the late summer is preceded by a peak in Fe(II) concentration and a small peak in NH_4 (Figs. 6a, b, 9a), which together with a shallower thermocline and N inputs from rain and senescent cyanobacteria, may have induced a second growth period for phytoplankton.

Filamentous cyanobacteria peak in abundance and biomass during the earlier part of the summer (25 and 28 μg C L^{-1} on 20 June and 20 July respectively). *Aphanizomenon* sp., *Nodularia spumigena,* and *Anabaena* sp. are the main representative species identified. *Anabaena* sp. has been described to produce the siderophore schizokinen in response to iron stress (Clarke et al., 1987) as well as the cyanotoxin microcystein that also has siderophore type characteristics (Kaebernick and Neilan, 2006; Utkilen and Gjolme, 1995; Humble et al., 1997). Further, Stolte et al. (2006) observed that cyanotoxin production by *Nodularia spumigena* increases during incubations with combined additions of DOM and Fe. The toxin production of *Nodularia spumigena* could be a response to increase metal bioavailability in media with strong DOM-metal complexation, where the dissolved iron concentrations are high, but the actual concentration of the bioavailable inorganic iron species (Fe') is low. Moreover, the pico-cyanobacteria

such as *Synechococcus* sp. were not assessed in our study, but can contribute up to 80% of the cyanobacterial biomass (Stal et al., 2003). *Synechococcus* sp. is a ubiquitous marine cyanobacterium and known as a producer of strong iron siderophores (Wilhelm et al., 1996) that can be photolabile (Barbeau et al., 2003). While the main proportion of iron complexing substances in coastal seawater, and especially in the Baltic Sea, is dissolved organic matter such as humic and fulvic acids (Hagström et al., 2001; Öztürk et al., 2002b; Rose and Waite, 2003), which can be present in truly dissolved or colloidal form (Hassellöv, 2005; Wells, 1998), here the relative importance of locally produced siderophores increases with the decrease of total ligand concentrations. We suggest that local production of iron chelators may hence counteract the overall loss of humic substances by processes such as photoreduction and export over the summer that mainly enter the Baltic Sea via high fresh water input during spring time (Hagström et al., 2001; Bergström et al., 2001). What percentage of the total iron binding ligands detected here is supplied by *Anabaena* sp., *Nodularia spumigena,* or also *Synechococcus* sp. remains unclear, but given the high conditional stability constants of some siderophore iron ligands (Witter et al., 2000) it seems plausible that the increase in iron-ligand complex stabilities was at least in part driven by cyanobacterial toxin and thus ligand production. Stolte and co-workers (2006) conclude that iron concentrations in the Baltic Sea are sufficient for cyanobacterial growth, but that species composition could be affected by species specific iron acquisition strategies. Our observations of abundance and successive growth of *Aphanizomenon* sp., *Nodularia spumigena*, and *Anabaena* sp. at Gotland Deep during the 2007 summer match this hypothesis, considering that the latter two are toxin and iron ligand producers.

4.3.2 Loss of Fe(III) organic ligands and H_2O_2 production

In general, loss of metal complexing ligands can be due to phytoplankton uptake or irreversible disintegration during photoreduction of the iron-ligand complex (Waite and Morel, 1984). Here iron binding ligands were diminished into a state of ligand deficiency with regard to dissolved iron concentrations between mid June and early August

(Fig. 7b). This will ultimately result in loss of iron from the system, since un-complexed iron will rapidly form iron-hydroxides and precipitate. Thus, also any Fe(II) produced during this time period would be lost from the system after re-oxidation, if it was not taken up by phytoplankton or retained in form of Fe(II)-organic complexes, which are not detected by Fe(III)-organic ligand titrations. Despite the increase in total iron towards the end of the summer the dissolved iron concentrations in our study progressively decrease (Fig. 7a). The particulate iron may in part be composed of iron taken up into phytoplankton cells, of which in this ecosystem a considerable fraction was initially supplied in form of Fe(II). Further, the decrease of iron binding ligands in the surface waters during the summer will also be driven by iron utilization from iron-ligand complexes, which can include iron-ligand uptake or loss of ligands after reduction of the iron-ligand complex at the cell surface (Morel et al., 2008; Shaked et al., 2005). Ligand-metal charge transfer and successive release of Fe(II) from the organic complex during photoreduction can further result in ligand destruction by irradiance, which results in H_2O_2 production (Abele-Oeschger et al., 1997). Our data show that H_2O_2 values coincide with Fe(II) in the upper part of the water column and indicate such mechanism (Figs. 3f, 4f, 5e). H_2O_2 concentrations >200 nmol L^{-1} can affect Fe(II) oxidation rates above present O_2 concentrations in surface seawater (Santana-Casiano et al., 2006). Such concentrations however were only measured once (20 July, Fig. 4f) at 40 m depth in a Gotland Deep profile, where no detectable Fe(II) was present. Presence of H_2O_2 at water depths below the euphotic zone also indicates that processes other than subsequent H_2O_2 formation after superoxide production from photodegradation of organic matter (Abele-Oeschger et al., 1997) must be responsible for H_2O_2 production in these waters. Hydrogen peroxide can also be a product of superoxide production on cell surfaces, cellular leakage processes and superoxide dismutase activity, and thus gets directly involved in cell surface iron reduction and uptake mechanisms (Pamatmat, 1997; Fan, 2008; Kustka et al., 2005).

We aimed to further elucidate the interrelations of H_2O_2, Fe(II), and different phytoplankton groups by performing deck incubations of water that was free of any phyto-

plankton (0.2 μm filtered), enriched in heterocystous cyanobacteria or depleted thereof, and untreated (Fig. 11a, b). We did not directly observe differences in H_2O_2 production in either phytoplankton group, however the similarity in all treatments except the 0.2 μm filtered fraction suggest that H_2O_2 is largely produced abiotic and mediated by eukaryotic or non-heterocystous cyanobacterial phytoplankton. Heterocystous cyanobacteria do not specifically consume H_2O_2 (Fig. 11a). Similar, Fe(II) production is mainly contributed by photoreduction of organic matter, but also reoxidized when H_2O_2 levels are high, such as in the 0.2 μm filtered fraction where no consumers in form of any phytoplankton are present. Further, Fe(II) is readily consumed by heterocystous cyanobacteria, as indicated by the low Fe(II) concentrations in the incubations that were enriched in cyanobacteria and the progressive increase in Fe(II) in the treatments that were depleted of this group (Fig. 11b). Recognizing limitations of this small data set from the shipboard incubations, we suggest that H_2O_2 can play a crucial role in iron redox cycling and phytoplankton iron uptake in Baltic waters, albeit cyanobacteria themselves apparently do not directly increase the Fe(II) pool in the water, as was observed for diatom species in the Southern Ocean (Rijkenberg et al., 2008).

4.3.3 Factors controlling Fe(II) concentrations

Comparing irradiation, dissolved oxygen, hydrogen peroxide, and Fe(II) concentrations over the course of the summer at Gotland Deep suggest that on 2 August the combination of the lowest O_2 concentration during the summer (605 μmol L^{-1}) and significantly less H_2O_2 (61 nmol L^{-1} vs. 161 nmol L^{-1}) than during the previous cruise (20 July) allowed for high Fe(II) levels at that time (Fig. 10). However, oxygen present still dominates Fe(II) oxidation rates (Santana-Casiano et al., 2006), and half-life's were rapid throughout the summer (0.04–0.32 min^{-1}), not differing much between these two dates. Further, the fact that irradiation was lowest of all cruises at this station together imply a different cause of the high Fe(II) values during 2 August. Rain deposition has been identified as a major source of Fe(II) to seawater (Kieber et al., 2001) and recently also for Fe(II) binding ligands (Willey et al., 2008; Kieber et al., 2005). The study period was

subject to frequent rain events and especially the cruise on 2 August (Gotland Deep) and 4 July (Landsort Deep) were preceded with periods of significant rain deposition. Therefore, we imply that Fe(II) deposited or produced during this period may have been maintained at elevated levels by hampered Fe(II) oxidation rates due to organic Fe(II) complexation. It should be noted, that the profile on 4 July (Landsort Deep, Fig. 5e) was measured at mid-night. While the Nordic summer at this latitude (58°36′ N) results in residual light throughout most of the night (sunset 21:42 local time), the light intensity even at a few meters water depth and estimated Fe(II) oxidation rates not considering organic complexation would not allow for the detected Fe(II) concentrations to be present at mid-night. Fe(II) half-life's calculated for surface water at LD approximate 1 s^{-1} and 2.9 min^{-1} at 20 m on 4 July. Nevertheless, 0.22–0.39 nmol L^{-1} Fe(II) were measured in the mixed layer of this station and must be maintained in solution by organic ligand binding, or a combination thereof with cell surface reduction mechanisms (O'Sullivan et al., 1991; Shaked et al., 2004; Kustka et al., 2005). The second Fe(II) maximum between 40–60 m depth is of different origin but will be discussed in more detail elsewhere (see Sect. 4.2).

The Fe(II) concentrations in our study account for up to 20% of the dissolved iron concentration at 5 m depth and thus contribute a significant fraction to the dissolved iron pool, and greatly enhance the fraction of bioavailable iron. Roy et al. (2008) report Fe(II) concentrations in the HNLC western subarctic Pacific that account for up to 50% of the dissolved iron fraction and suggest that ligands containing amine or thiol functional groups may be responsible for Fe(II) complexation. This would be the case for copper specific ligands produced by phytoplankton to mitigate elevated copper stress (Dupont et al., 2004). Copper concentrations in surface water of this region of the Baltic Sea generally account for up to 10 nmol L^{-1} (Pohl and Hennings, 1999, 2005) and copper complexation by thiol groups has been observed in Baltic waters (Breitbarth et al., unpublished data). It is possible that copper ligand production has the side effect of Fe(II) complexation and thus maintains Fe(II) in seawater by slowing oxidation rates (Roy et al., 2008), therefore affecting the overall bioavailability of iron that otherwise is

low due to the strong organic complexation and insufficient Fe' concentrations to fuel growth of large phytoplankton cells. Such a mechanism though remains to be validated for the Baltic Sea.

Alternatively, cyanobacteria aggregates could create low pH and low O_2 microenvironments during darkness that greatly enhance iron solubility as suggested recently by Ploug (2008). Such mechanism could supplement the utilization of Fe(II) during daytime photoreduction and maybe even enhance the half life of Fe(II) at night. However, the frequent wind driven mixing observed during the 2007 summer season prevented surface accumulation and large aggregate formation of cyanobacteria, which would be required to generate such microenvironments.

4.3.4 Standing stock and significance of Fe(II) for cyanobacterial growth

Fe(II) in Baltic Sea surface waters apparently is persistent at relatively high standing stocks throughout extended periods of time. Overall, the DGT and the Fe(II) profiles agree well on average concentrations of ~0.5 nmol L^{-1} at the surface and ~0.25 nmol L^{-1} at 5–10 m depth (Figs. 4e, f, 5e, f, 8). Next to inorganic iron species (Fe'), which only exists at picomolar levels (Fig. 7b) and potentially also low molecular weight bound iron that is labile to DGT, Fe(II) ions are permeating through the DGT membrane and diffusive gel layer. Our measurements propose that the main fraction of this DGT collected and presumably bioavailable iron is supplied in form of Fe(II). The disagreement of the two sampling techniques at 120 m (DGT profile 20 July–14 August, Fig. 8b) indicates that while both techniques detect ferric ions, DGT may also detect iron sulfides, which intermediately can be present at this depth, if their clusters are still small enough to permeate the DGT membrane.

The cellular iron quota of Baltic Sea nitrogen fixing cyanobacteria is ca. 100 μmol Fe:mol C (data from Gotland deep 2007, Walve unpublished) and thus results in a minimum cellular bound iron concentration of 0.23 nmol L^{-1} at the maximum cyanobacterial biomass of 2.32 μmol C L^{-1} (20 July). Using the cyanobacterial C fixation rate in (Walve and Larsson, 2007) and assuming 50% goes into growth, the iron requirement of het-

erocystous cyanobacteria is ca 1 nmol L^{-1} (0.017 nmol L^{-1} day^{-1}) for the two month growth period from 24 May to 20 July. Considering a 5–10 fold lower Fe demand for non-N-fixing phytoplankton than for N_2 fixing cyanobacteria (Kustka et al., 2003a), and an approximate C fixation rate of 30 μg C L-1 day^{-1} (Johansson et al., 2004) a rough estimation of the iron uptake during the same growth period ranges from 1.4–2.9 nmol L^{-1} (0.025–0.05 nmol L^{-1} day^{-1}). A large part of this uptake is recycled in the surface layer, and a small fraction lost by sedimentation. Half saturation constants with respect to inorganic iron reported for growth of the cyanobacteria *Microcystis aeruginosa* and *Planktothrix agardhii* were 0.14 and 0.31 nmol L^{-1}, respectively (Nagai et al., 2007). Diatom species of the genus *Thalassiosira* have Fe' half saturation constants to sustain their growth of 0.004–0.068 nmol L^{-1} (Sunda and Huntsman, 1995). Assuming similar requirements for the cyanobacteria and the eukaryotic phytoplankton present in the Baltic Sea, the standing stock of bioavailable iron of 0.25 nmol L^{-1}–0.5 nmol L^{-1} in the euphotic zone is contributing a significant proportion of the iron demand to fuel primary production and nitrogen fixation in these waters.

5 Conclusions

Overall, nutrient stoichiometry (Fig. 9) suggest that classic N-limitation (DIN:DIP ~0.5, 24 May) initiate the cyanobacterial bloom development. The ratio of dissolved iron concentrations to total phosphate and to dissolve inorganic nitrogen exceed those in oceanic regions by 2–3 and 3–4 orders of magnitude, respectively (Franck et al., 2003). However, the relatively high iron concentrations compared to macronutrients may not be directly accessible to phytoplankton. Thus, Fe(II) appears a major role in iron acquisition by phytoplankton, namely diazotrophic cyanobacteria, in the Baltic Sea. The photochemistry of this micronutrient further also counteracts losses by colloid and particle formation of bioavailable iron in the LMW fraction during bloom development, given that such a mechanism as identified for other trace metals also affects iron biogeochemistry in the Baltic Sea (Ingri et al., 2004). We conclude that the Baltic Proper is a stoichio-

metrically low nutrient – high iron system and that a large fraction of the bioavailable iron is supplied via Fe(II). This however is supplied via a combination of photochemical processes and rainwater deposition in surface water and apparently maintained to some extent by organic-Fe(II) complexation. Wind driven mixing does not reach the oxic-anoxic interface during summer time, ruling out Fe(II) and PO_4 rich deep water as source of nutrients for cyanobacterial bloom development.

Acknowledgements. The authors are very grateful to Murat V. Ardelan for lending his FIA system. K. N'dungu, H. Paulava, and R. Rentz helped at sea. Special thanks to P. Croot and C. Neill for the use of their FIA data acquisition program. Thanks also to the staff at the Department of Systems Ecology, Stockholm University, for analyzing nitrogen, phosphorus, chlorophyll, oxygen, and hydrogen sulfide. Meteorological data were provided by the Swedish Meteorological and Hydrological Institute (SMHI) and we acknowledge the help of E.-M. Wingqvist. This work was supported by Formas Grant No: 217-2005-1879 awarded to J. Ingri, M. Hassellöv, et al. E. Breitbarth further acknowledges a stipend from the Division of Applied Geology at Luleå University of Technology and support from the Gothenburg Marine Research Center. L. Hoffmann was supported by a DAAD fellowship. Stockholm Marine Research Center is thanked for subsidized access to the research vessel *Fyrbyggaren*.

References

Abele-Oeschger, D., Tüg, H., and Röttgers, R.: Dynamics of UV-driven hydrogen peroxide formation on an intertidal sandflat, Limnol. Oceanogr., 42, 1406–1415, 1997.

Anderson, M. A. and Morel, F. M. M.: The Influence of Aqueous Iron Chemistry on the Uptake of Iron by the Coastal Diatom *Thalassiosira weissflogii*, Limnol. Oceanogr., 27, 789–813, 1982.

Barbeau, K., Rue, E. L., Trick, C. G., Bruland, K. T., and Butler, A.: Photochemical reactivity of siderophores produced by marine heterotrophic bacteria and cyanobacteria based on characteristic Fe(III) binding groups, Limnol. Oceanogr., 48, 1069–1078, 2003.

Bergström, S., Alexandersson, H., Carlsson, B., Josefsson, W., Karlsson, K.-G., and Westring, G.: Climate and hydrology of the Baltic Basin, in: Ecological Studies. A systems analysis of the Baltic Sea, Ecol. Stud., 148, 75–112, 2001.

Boyd, P. W., Jickells, T., Law, C. S., Blain, S., Boyle, E. A., Buesseler, K. O., Coale, K. H., Cullen, J. J., de Baar, H. J. W., Follows, M., Harvey, M., Lancelot, C., Levasseur, M., Owens, N. P. J., Pollard, R., Rivkin, R. B., Sarmiento, J., Schoemann, V., Smetacek, V., Takeda, S., Tsuda, A., Turner, S., and Watson, A. J.: Mesoscale Iron Enrichment Experiments 1993-2005: Synthesis and Future Directions, Science, 315, 612–617, doi:10.1126/science.1131669, 2007.

Brügmann, L., Bernard, P. C., and Vangrieken, R.: Geochemistry of Suspended Matter from the Baltic Sea 2 – Results of Bulk Trace-Metal Analysis by AAS, Mar. Chem., 38, 303–323, 1992.

Brügmann, L., Hallberg, R., Larsson, C., and Loffler, A.: Trace metal speciation in sea and pore water of the Gotland Deep, Baltic Sea, 1994, Appl. Geochem., 13, 359–368, 1998.

Bruland, K. W., Lohan, M. C., Heinrich, D. H., and Karl, K. T.: Controls of Trace Metals in Seawater, in: Treatise on Geochemistry, Pergamon, Oxford, 23–47, 2003.

Clarke, S. E., Stuart, J., and Sandersloehr, J.: Induction of Siderophore Activity in *Anabaena spp* and Its Moderation of Copper Toxicity, Appl. Environ. Microb., 53, 917–922, 1987.

Croot, P. L. and Johansson, M.: Determination of iron speciation by cathodic stripping voltammetry in seawater using the competing ligand 2-(2-thiazolylazo)-p-cresol (TAC), Electroanalysis, 12, 565–576, 2000.

Croot, P. L., Bowie, A. R., Frew, R. D., Maldonado, M. T., Hall, J. A., Safi, K. A., La Roche, J., Boyd, P. W., and Law, C. S.: Retention of dissolved iron and Fe-II in an iron induced Southern Ocean phytoplankton bloom, Geophys. Res. Lett., 28, 3425–3428, 2001.

Croot, P. L. and Laan, P.: Continuous shipboard determination of Fe(II) in polar waters using flow injection analysis with chemiluminescence detection, Anal. Chim. Acta, 466, 261–273, 2002.

Croot, P. L., Bluhm, K., Schlosser, C., Streu, P., Breitbarth, E., Frew, R. D., and Ardelan, M. V.: Cycling of Fe(II) in Southern Ocean Iron Mesoscale Enrichment Experiments: EIFEX and SOFEX, Geophys. Res. Lett., 35, L19606. doi:19610.11029/12008GL035063, 2008.

Dahlqvist, R., Zhang, H., Ingri, J., and Davison, W.: Performance of the diffusive gradients in thin films technique for measuring Ca and Mg in freshwater, Anal. Chim. Acta, 460, 247–256, 2002.

Davison, W. and Zhang, H.: In-Situ Speciation Measurements of Trace Components in Natural-Waters Using Thin-Film Gels, Nature, 367, 546–548, 1994.

de Baar, H. J. W., Boyd, P. W., Coale, K. H., Landry, M. R., Tsuda, A., Assmy, P., Bakker, D. C. E., Bozec, Y., Barber, R. T., Brzezinski, M. A., Buesseler, K. O., Boye, M., Croot, P. L.,

Gervais, F., Gorbunov, M. Y., Harrison, P. J., Hiscock, W. T., Laan, P., Lancelot, C., Law, C. S., Levasseur, M., Marchetti, A., Millero, F. J., Nishioka, J., Nojiri, Y., van Oijen, T., Riebesell, U., Rijkenberg, M. J. A., Saito, H., Takeda, S., Timmermans, K. R., Veldhuis, M. J. W., Waite, A. M., and Wong, C. S.: Synthesis of iron fertilization experiments: From the Iron Age in the Age of Enlightenment, J. Geophys. Res., 110, C09S16, doi:10.1029/2004JC002601, 2005.

Dupont, C. L., Nelson, R. K., Bashir, S., Moffett, J. W., and Ahner, B. A.: Novel copper-binding and nitrogen-rich thiols produced and exuded by Emiliania huxleyi, Limnol. Oceanogr., 49, 1754–1762, 2004.

Fan, S.-M.: Photochemical and biochemical controls on reactive oxygen and iron speciation in the pelagic surface ocean, Mar. Chem., 109, 152–164, 2008.

Finni, T., Kononen, K., Olsonen, R., and Wallstrom, K.: The history of cyanobacterial blooms in the Baltic Sea, AMBIO, 30, 172–178, 2001.

Fonselius, S., Dyrssen, D., and Yhlen, B.: Determination of hydrogen sulfide, in: Methods of Seawater Analysis, edited by: Grasshoff, K., Kremling, K., and Ehrhard, M., Wiley-VCH, 91–100, 1999.

Forsberg, J., Dahlqvist, R., Gelting-Nystrom, J., and Ingri, J.: Trace metal speciation in brackish water using diffusive gradients in thin films and ultrafiltration: Comparison of techniques, Environ. Sci. Technol., 40, 3901–3905, 2006.

Franck, V. M., Bruland, K. W., Hutchins, D. A., and Brzezinski, M. A.: Iron and zinc effects on silicic acid and nitrate uptake kinetics in three high-nutrient, low-chlorophyll (HNLC) regions, Mar. Ecol.-Prog. Ser., 252, 15–33, 2003.

Gelting, J., Breitbarth, E., Walve, J., Norblad, F., Hassellöv, M., Stolpe, B., and Ingri, J.: Physicochemical fractionation of iron during transport from fresh to marine waters, Biogeosciences Discuss., in preparation, 2009a.

Gelting, J., Breitbarth, E., Walve, J., Norblad, F., Hassellöv, M., Stolpe, B., and Ingri, J.: Seasonal variation of iron speciation in low salinity surface water in the Baltic Sea, Biogeosciences Discuss., in preparation, 2009b.

Gerringa, L. J. A., Herman, P. M. J., and Poortvliet, T. C. W.: Comparison of the linear Van den Berg/Ruzic transformation and a non-linear fit of the Langmuir isotherm applied to Cu speciation data in the estuarine environment, Mar. Chem., 48, 131–142, 1995.

Hagström, A., Azam, F., Kuparinen, J., and Zweifel, U.-L.: Pelagic plankton growth and resource limitations in the Baltic Sea, in: Ecological Studies. A systems analysis of the Baltic Sea, Ecol. Stud., 148, 177–210, 2001.

Hassellöv, M.: Relative molar mass distributions of chromophoric colloidal organic matter in coastal seawater determined by Flow Field-Flow Fractionation with UV absorbance and fluorescence detection, Mar. Chem., 94, 11–123, 2005.
Humble, A. V., Gadd, G. M., and Codd, G. A.: Binding of copper and zinc to three cyanobacterial microcystins quantified by differential pulse polarography, Water Res., 31, 1679–1686, 1997.
Hutchins, D. A., DiTullio, G. R., Zhang, Y., and Bruland, K. W.: An iron limitation mosaic in the California upwelling regime, Limnol. Oceanogr., 43, 1037–1054, 1998.
Ingri, J., Nordling, S., Larsson, J., Ronnegard, J., Nilsson, N., Rodushkin, I., Dahlqvist, R., Andersson, P., and Gustafsson, O.: Size distribution of colloidal trace metals and organic carbon during a coastal bloom in the Baltic Sea, Mar. Chem., 91, 117–130, 2004.
Johansson, M., Gorokhova, E., and Larsson, U.: Annual variability in ciliate community structure, potential prey and predators in the open northern Baltic Sea proper, J. Plankton Res., 26, 67–80, doi:10.1093/plankt/fbg115, 2004.
Kaebernick, M. and Neilan, B. A.: Ecological and molecular investigations of cyanotoxin production, FEMS Microbiol. Ecol., 35, 1–9, 2006.
Kahru, M., Savchuk, O. P., and Elmgren, R.: Satellite measurements of cyanobacterial bloom frequency in the Baltic Sea: interannual and spatial variability, Mar. Ecol. Prog. Ser., 343, 15–23, doi:10.3354/meps06943, 2007.
Kieber, R. J., Williams, K., Willey, J. D., Skrabal, S., and Avery, G. B.: Iron speciation in coastal rainwater: concentration and deposition to seawater, Mar. Chem., 73, 83–95, 2001.
Kieber, R. J., Skrabal, S. A., Smith, B. J., and Willey, J. D.: Organic complexation of Fe(II) and its impact on the redox cycling of iron in rain, Environ. Sci. Technol., 39, 1576–1583, doi:10.1021/es040439h, 2005.
King, D. W., Aldrich, R. A., and Charnecki, S. E.: Photochemical Redox Cycling of Iron in Nacl Solutions, Mar. Chem., 44, 105–120, 1993.
Kononen, K., Kuparinen, J., Mäkelä, K., Laanemets, J., Pavelson, J., and Nômmann, S.: Initiation of cyanobacterial blooms in a frontal region at the entrance to the Gulf of Finland, Baltic Sea, Limnol. Oceanogr., 41, 98–112, 1996.
Kuma, K., Nakabayashi, S., Suzuki, Y., Kudo, I., and Matsunaga, K.: Photo-Reduction of Fe (III) by Dissolved Organic-Substances and Existence of Fe (II) in Seawater During Spring Blooms, Mar. Chem., 37, 15–27, 1992.
Kuma, K., Nakabayashi, S., and Matsunaga, K.: Photoreduction of Fe(III) by Hydroxycarboxylic Acids in Seawater, Water Res., 29, 1559–1569, 1995.

Kustka, A., Carpenter, E. J., and Sanudo-Wilhelmy, S. A.: Iron and marine nitrogen fixation: progress and future directions, Res. Microbiol., 153, 255–262, 2002.
Kustka, A., Sanudo-Wilhelmy, S., Carpenter, E. J., Capone, D. G., and Raven, J. A.: A revised estimate of the iron use efficiency of nitrogen fixation, with special reference to the marine cyanobacterium *Trichodesmium* spp. (Cyanophyta), J. Phycol., 39, 12–25, 2003a.
Kustka, A. B., Sanudo-Wilhelmy, S. A., Carpenter, E. J., Capone, D., Burns, J., and Sunda, W. G.: Iron requirements for dinitrogen- and ammonium-supported growth in cultures of Trichodesmium (IMS 101): Comparison with nitrogen fixation rates and iron: carbon ratios of field populations, Limnol. Oceanogr., 48, 1869–1884, 2003b.
Kustka, A. B., Shaked, Y., Milligan, A. J., King, D. W., and Morel, F. M. M.: Extracellular production of superoxide by marine diatoms: Contrasting effects on iron redox chemistry and bioavailability, Limnol. Oceanogr., 50, 1172–1180, 2005.
Larsson, U., Hajdu, S., Walve, J., and Elmgren, R.: Baltic Sea nitrogen fixation estimated from the summer increase in upper mixed layer total nitrogen, Limnol. Oceanogr., 46, 811–820, 2001.
Lewis, E. and Wallace, D. W. R.: Program Developed for CO_2 System Calculations. ORNL/CDIAC-105. Carbon Dioxide Information Analysis Center, Oak Ridge National Laboratory, U.S. Department of Energy, Oak Ridge, Tenessee, USA, 1998.
Meier, H. E. M.: Modeling the pathways and ages of inflowing salt- and freshwater in the Baltic Sea, Estuar. Coast. Shelf S., 74, 610–627, doi:10.1016/j.ecss.2007.05.019, 2007.
Menden-Deuer, S. and Lessard, E. J.: Carbon to volume relationships for dinoflagellates, diatoms, and other protist plankton, Limnol. Oceanogr., 45, 569–579, 2000.
Millero, F. J., Sotolongo, S., and Izaguirre, M.: The oxidation kinetics of Fe(II) in seawater, Geochim. Cosmochim. Acta, 51, 793–801, 1987.
Millero, F. J. and Sotolongo, S.: The oxidation of Fe(II) with H2O2 in seawater, Geochim. Cosmochim. Acta, 53, 1867–1873, 1989.
Moffett, J. W., Goeffert, T. J., and Naqvi, S. W. A.: Reduced iron associated with secondary nitrite maxima in the Arabian Sea, Deep-Sea Res. I, 54, 1341–1349, 2007.
Morel, F. M. M., Kustka, A. B., and Shaked, Y.: The role of unchelated Fe in the iron nutrition of phytoplankton, Limnol. Oceanogr., 53, 400–404, 2008.
Nagai, T., Imai, A., Matsushige, K., Yokoi, K., and Fukushima, T.: Dissolved iron and its speciation in a shallow eutrophic lake and its inflowing rivers, Water Res., 41, 775–784, 2007.
O'Sullivan, D. W., Hanson, A. K., Miller, W. L., and Kester, D. R.: Measurement of Fe(II) in

surface water of the equatorial Pacific, Limnol. Oceanogr., 36, 1727–1741, 1991.
Öztürk, M., Steinnes, E., and Sakshaug, E.: Iron speciation in the Trondheim Fjord from the perspective of iron limitation for phytoplankton, Estuar. Coast. Shelf S., 55, 197–212, 2002a.
Öztürk, M., Steinnes, E., and Sakshaug, E.: Iron Speciation in the Trondheim Fjord from the Perspective of Iron Limitation for Phytoplankton, Estuar. Coast. Shelf S., 55, 197–212, 2002b.
Pamatmat, M. M.: Non-photosynthetic oxygen production and non-respiratory oxygen uptake in the dark: a theory of oxygen dynamics in plankton communities, Mar. Biol., 129, 735–746, 1997.
Ploug, H.: Cyanobacterial surface blooms formed by *Aphanizomenon* sp. and *Nodularia spumigena* in the Baltic Sea: Small-scale fluxes, pH, and oxygen microenvironments, Limnol. Oceanogr., 53, 914–921, 2008.
Pohl, C. and Hennings, U.: The effect of redox processes on the partitioning of Cd, Pb, Cu, and Mn between dissolved and particulate phases in the Baltic Sea, Mar. Chem., 65, 41–53, 1999.
Pohl, C. and Hennings, U.: The coupling of long-term trace metal trends to internal trace metal fluxes at the oxic-anoxic interface in the Gotland Basin (57 degrees 19, 20′ N; 20 degrees 03,00 ’ E) Baltic Sea, J. Marine Syst., 56, 207–225, doi:10.1016/j.jmarsys.2004.10.001, 2005.
Rijkenberg, M. J. A., Gerringa, L. J. A., Timmermans, K. R., Fischer, A. C., Kroon, K. J., Buma, A. G. J., Wolterbeek, B. T., and de Baar, H. J. W.: Enhancement of the reactive iron pool by marine diatoms, Mar. Chem., 109, 29–44, 2008.
Rodushkin, I. and Ruth, T.: Determination of trace metals in estuarine and sea-water reference materials by high resolution inductively coupled plasma mass spectrometry, J. Anal. Atom. Spectrom., 12, 1181–1185, 1997.
Rose, A. L. and Waite, T. D.: Chemiluminescence of luminol in the presence of iron(II) and oxygen: Oxidation mechanism and implications for its analytical use, Anal. Chem., 73, 5909–5920, 2001.
Rose, A. L. and Waite, T. D.: Kinetics of iron complexation by dissolved natural organic matter in coastal waters, Mar. Chem., 84, 85–103, doi:10.1016/s0304-4203(03)00113-0, 2003.
Roy, E. G., Wells, M. L., and King, D. W.: Persistence of iron(II) in surface waters of the western subarctic Pacific, Limnol. Oceanogr., 53, 89–98, 2008.
Rue, E. L. and Bruland, K. W.: Complexation of iron(III) by natural organic ligands in the Central

North Pacific as determined by a new competitive ligand equilibration/adsorptive cathodic stripping voltammetric method, Mar. Chem., 50, 117–138, 1995.
Santana-Casiano, J. M., Gonzalez-Davila, M., and Millero, F. J.: The role of Fe(II) species on the oxidation of Fe(II) in natural waters in the presence of O_2 and H_2O_2, Mar. Chem., 99, 70–82, 2006.
Sanudo-Wilhelmy, S. A., Kustka, A. B., Gobler, C. J., Hutchins, D. A., Yang, M., Lwiza, K., Burns, J., Capone, D. G., Ravenk, J. A., and Carpenter, E. J.: Phosphorus limitation of nitrogen fixation by *Trichodesmium* in the central Atlantic Ocean, Nature, 411, 66–69, 2001.
Shaked, Y., Kustka, A. B., Morel, F. M. M., and Erel, Y.: Simultaneous determination of iron reduction and uptake by phytoplankton, Limnol. Oceanogr.-Meth., 2, 137–145, 2004.
Shaked, Y., Kustka, A. B., and Morel, F. M. M.: A general kinetic model for iron acquisition by eukaryotic phytoplankton, Limnol. Oceanogr., 50, 872–882, 2005.
Stal, L. J., Staal, M., and Villbrandt, M.: Nutrient control of cyanobacterial blooms in the Baltic Sea, Aquat. Microb. Ecol., 18, 165–173, 1999.
Stal, L. J., Albertano, P., Bergman, B., von Brockel, K., Gallon, J. R., Hayes, P. K., Sivonen, K., and Walsby, A. E.: BASIC: Baltic Sea cyanobacteria. An investigation of the structure and dynamics of water blooms of cyanobacteria in the Baltic Sea - responses to a changing environment, Cont. Shelf Res., 23, 1695–1714, doi:10.1016/j.csr.2003.06.001, 2003.
Stolte, W., Balode, M., Carlsson, P., Grzebyk, D., Janson, S., Lips, I., Panosso, R., Ward, C. J., and Graneli, E.: Stimulation of nitrogen-fixing cyanobacteria in a Baltic Sea plankton community by land-derived organic matter or iron addition, Mar. Ecol. Prog. Ser., 327, 71–82, 2006.
Strady, E., Pohl, C., Yakushev, E. V., Kruger, S., and Hennings, U.: PUMP-CTD-System for trace metal sampling with a high vertical resolution. A test in the Gotland Basin, Baltic Sea, Chemosphere, 70, 1309–1319, 2008.
Sunda, W. G. and Huntsman, S. A.: Iron uptake and growth limitation in oceanic and coastal phytoplankton, Mar. Chem., 50, 189–206, 1995.
Sunda, W. G.: Bioavailability and Bioaccumulation of Iron in the Sea, in: The Biogeochemistry of Iron in Seawater, edited by: Turner, D. R. and Hunter, K. A., John Wiley and Sons Ltd., West Sussex, UK, 396 pp., 2001.
Utkilen, H. and Gjolme, N.: Iron-Stimulated Toxin Production in Microcystis-Aeruginosa, Appl. Environ. Microbiol., 61, 797–800, 1995.
Waite, T. D. and Morel, F. M. M.: Photoreductive dissolution of colloidal iron oxides in natural

waters, Environ. Sci. Technol., 18, 860–868, 1984.
Walve, J. and Larsson, U.: Blooms of Baltic Sea Aphanizomenon sp (cyanobacteria) collapse after internal phosphorus depletion, Aquat. Microb. Ecol., 49, 57–69, doi:10.3354/ame01130, 2007.
Wells, M. L. and Mayer, L. M.: The Photoconversion of Colloidal Iron Oxyhydroxides in Seawater, Deep-Sea Res. I, 38, 1379–1395, 1991.
Wells, M. L.: A neglected dimension, Nature, February 1998, 530–531, 1998.
Wilhelm, S. W., Maxwell, D. P., and Trick, C. G.: Growth, iron requirements, and siderophore production in iron-limited Synechococcus PCC 7002, Limnol. Oceanogr., 41, 89–97, 1996.
Willey, J. D., Kieber, R. J., Seaton, P. J., and Miller, C.: Rainwater as a source of Fe(II)-stabilizing ligands to seawater, Limnol. Oceanogr., 53, 1678–1684, 2008.
Witter, A. E., Hutchins, D. A., Butler, A., and Luther III, G. W.: Determination of conditional stability constants and kinetic constants for strong model Fe-binding ligands in seawater, Mar. Chem., 69, 1–17, 2000.
Yuan, J. C. and Shiller, A. M.: Determination of subnanomolar levels of hydrogen peroxide in seawater by reagent-injection chemiluminescence detection, Anal. Chem., 71, 1975–1980, 1999.
Zhang, H. and Davison, W.: Performance-Characteristics of Diffusion Gradients in Thin-Films for the in-Situ Measurement of Trace-Metals in Aqueous-Solution, Anal. Chem., 67, 3391–3400, 1995.
Zhang, H. and Davison, W.: Diffusional characteristics of hydrogels used in DGT and DET techniques, Anal. Chim. Acta, 398, 329–340, 1999.

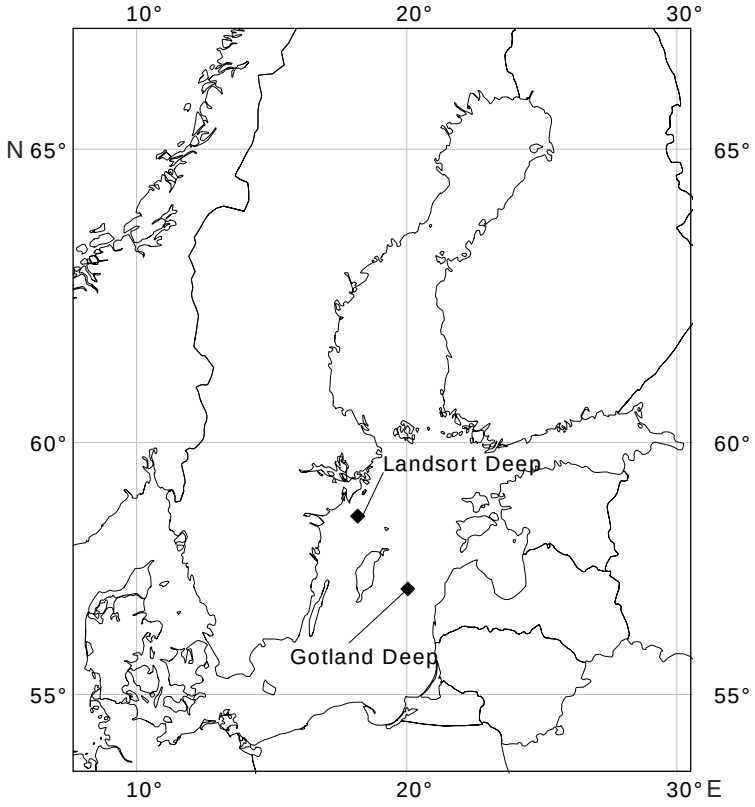

Fig. 1. Map of the Baltic Sea with the two sampling sites: Landsort Deep (58°36′ N, 18°14′ E) and Gotland Deep (57°18′ N; 20°04′ E).

BGD

6, 3803–3850, 2009

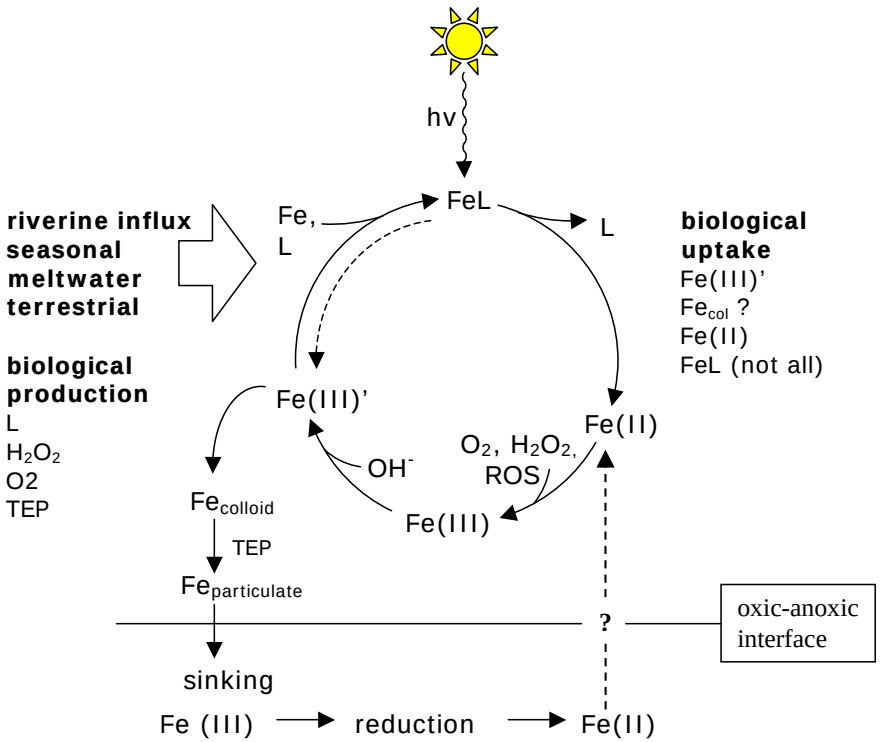

Fig. 2. Proposed Fe cycle for the Baltic Sea at Gotland Deep (image modified based on Sunda, 2001 and Croot et al., 2005).

BGD
6, 3803–3850, 2009

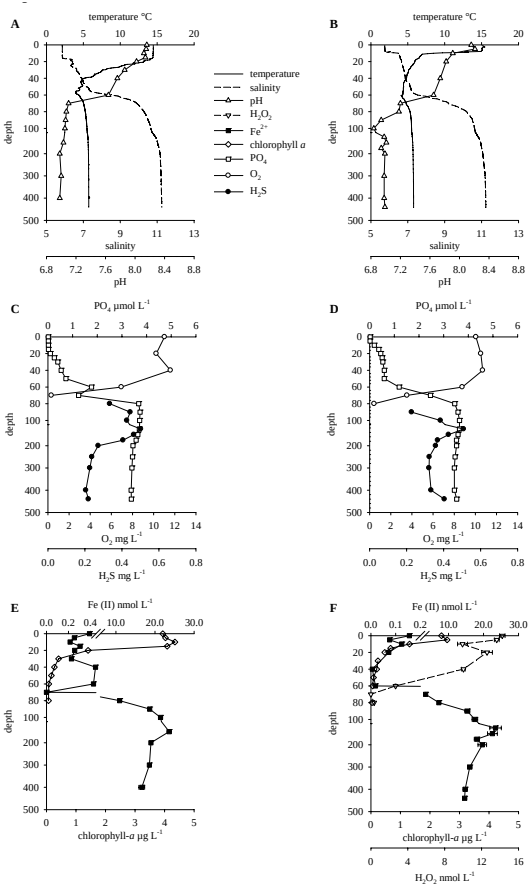

Fig. 3. Depth profiles of parameters measured throughout the water column at Landsort Deep. Note that the x-axis is stretched for better visibility of surface patterns between 0 and 100 m depth. **(A)** and **(B)** illustrate temperature in °C, salinity (PSU), and pH. **(C)** and **(D)** show dissolved oxygen (O_2), hydrogen sulfide (H_2S), and phosphate (PO_4). **(E)** and **(F)** show chlorophyll–*a*, iron(II), and hydrogen peroxide (H_2O_2, **(F)** only). Sampling dates were 4 July (A, C, and E) and 1 August 2007 (B, D, and F).

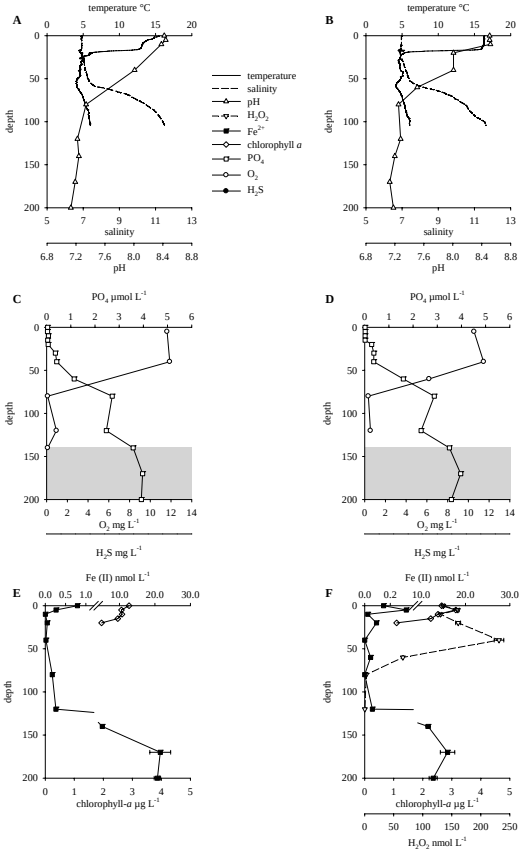

Fig. 4. Depth profiles of parameters measured throughout the water column at Gotland Deep. **(A)** and **(B)** illustrate temperature in °C, salinity (PSU), and pH. **(C)** and **(D)** show dissolved oxygen (O_2) and phosphate (PO_4). Hydrogen sulfide (H_2S) was not analytically measured and the grey zone indicates H_2S smell of the sampled water. **(E)** and **(F)** show chlorophyll−*a*, iron(II), and hydrogen peroxide (H_2O_2, F only). Sampling dates were 20 June (A, C, and E) and 20 July 2007 (B, D, and F).

BGD
6, 3803–3850, 2009

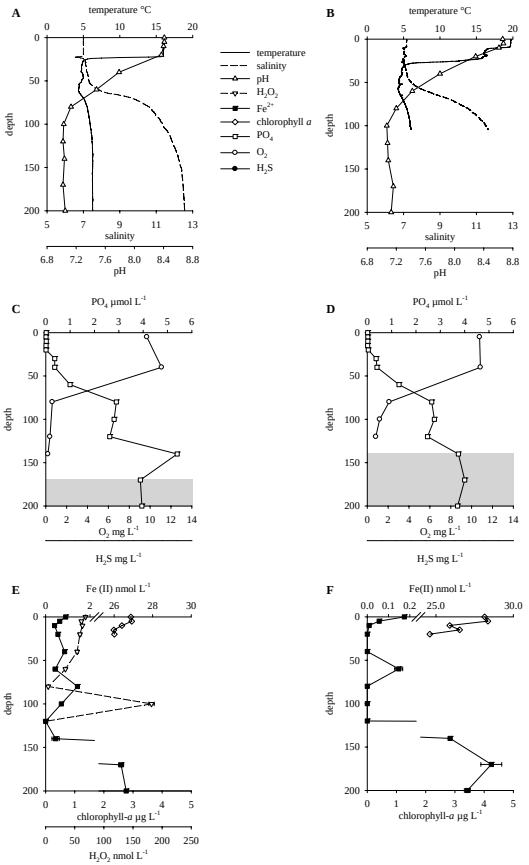

Fig. 5. Depth profiles of parameters measured throughout the water column at Gotland Deep. **(A)** and **(B)** illustrate temperature in ˚C, salinity (PSU), and pH. **(C)** and **(D)** show dissolved oxygen (O_2) and phosphate (PO_4). Hydrogen sulfide (H_2S) was not analytically measured and the grey zone indicates H_2S smell of the sampled water. **(E)** and **(F)** show chlorophyll–*a*, iron(II), and hydrogen peroxide (H_2O_2, E only). Sampling dates were 2 August (A, C, and E) and 14 August 2007 (B, D, and F).

BGD
6, 3803–3850, 2009

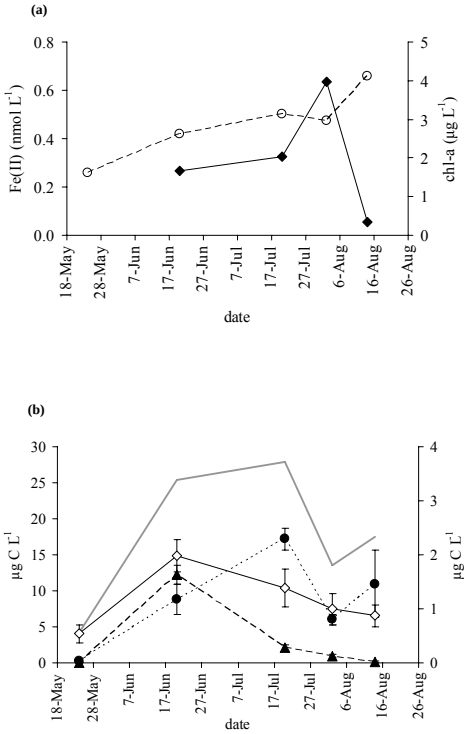

Fig. 6. **(a)** Fe(II) and chlorophyll–*a* (chl-*a*) measurements at 5 m depth over the course of the study period at Gotland Deep. Fe(II) is depicted by solid diamonds and chl-*a* is shown as open circles. **(b)** Evolution of heterocystous cyanobacteria in surface water (0–20 m depth) at Gotland Deep during the summer of 2007 expressed in μg C L^{-1}. Open diamonds indicate *Aphanizomenon*, solid circles show *Nodularia*, and solid triangles depict *Anabaena* (plotted on different scale on the right hand y-axis). The grey line shows the total biomass of heterocystous cyanobacteria. Error bars show standard deviations.

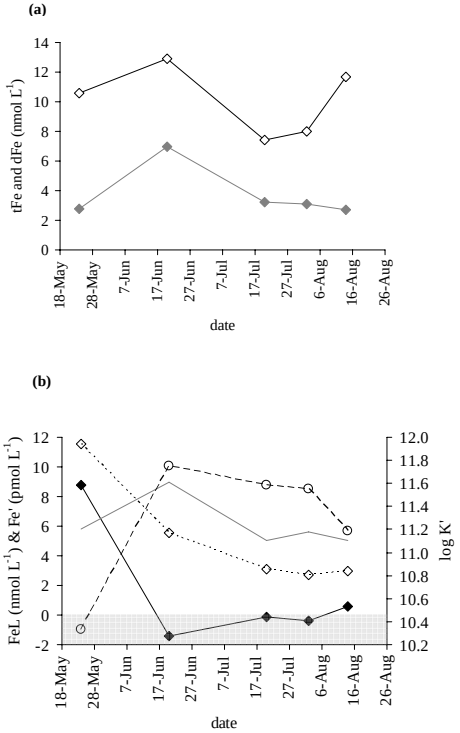

Fig. 7. (a) Development of total iron (tFe) and dissolved iron (0.2 μm filtered, dFe) during the study period at 5 m depth at Gotland Deep. Open diamonds are total iron and solid diamonds show dissolved iron. **(b)** Organic complexation of the dissolved iron fraction and inorganic iron species (Fe') during the different sampling occasions at Gotland Deep, 5 m depth. Open diamonds show the iron binding ligand concentrations; solid diamonds depict the concentration of excess ligands. The grey line shows the concentration of Fe'. Circles indicate the conditional stability constant with respect to Fe' (plotted on the right hand y-axis).

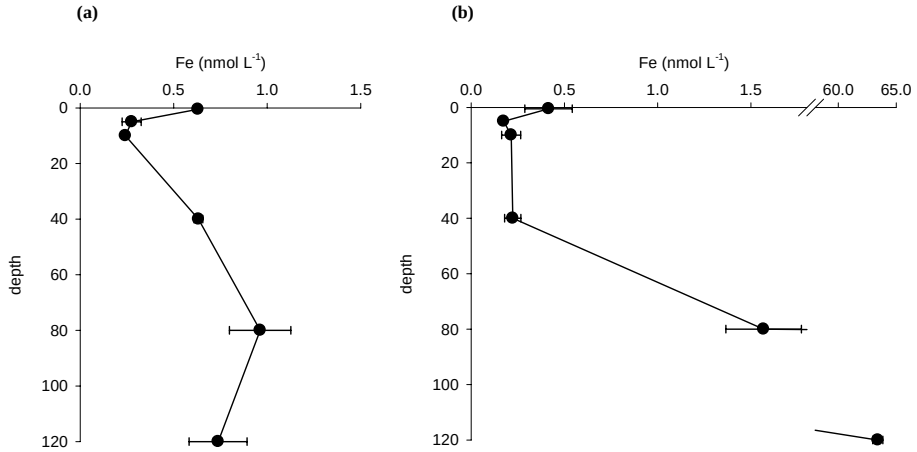

Fig. 8. (a) Profile of DGT measured iron in the top 120 m water depth at Gotland Deep during the time period 24 May–20 June, 2007. **(b)** Profile of DGT measured iron in the top 120 m water depth at Gotland Deep during the time period 20 July–14 August, 2007.

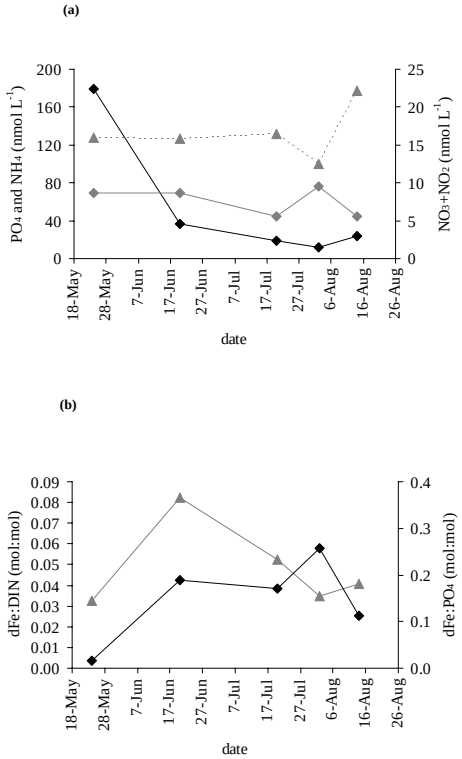

Fig. 9. **(a)** Development of macronutrients at 5 m water depth during the study at Gotland Deep. Phosphate (PO_4, black diamonds) and ammonia (NH_4, grey diamonds) are plotted on the left y-axis. NO_3 and NO_2 were measured together and are plotted on the right y-axis (grey triangle). **(b)** Macronutrient: dissolved iron stoichiometry at 5 m water depth at Gotland Deep. The ratio of dissolved inorganic nitrogen (DIN): dissolved iron (Fe) is shown by grey triangles (left y-axis). Phosphate (PO_4) : Fe stoichiometry is depicted by black diamonds (right y-axis).

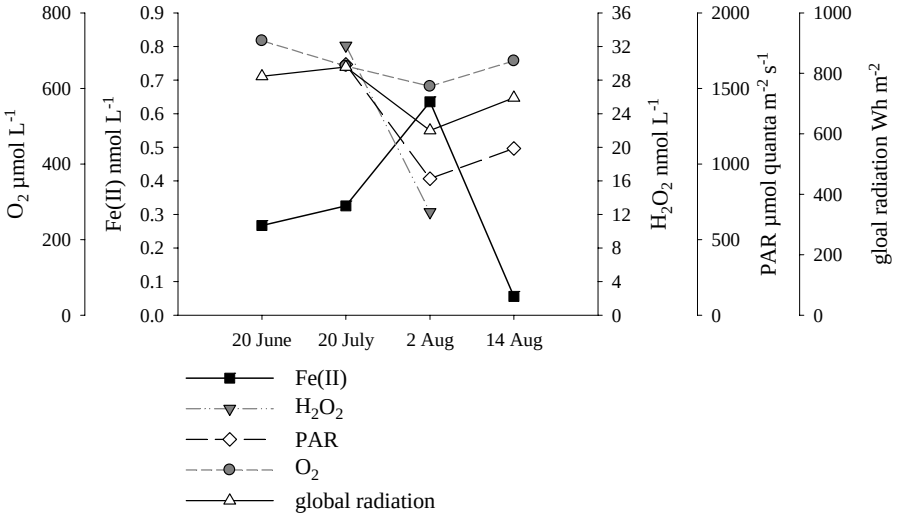

Fig. 10. Relationships of Fe(II), surface irradiance (photosynthetic active radiation – PAR) measured on board the ship during the Fe(II) cast, global radiation measured at the SMHI station Visby on Gotland, hydrogen peroxide (H_2O_2), and dissolved oxygen (O_2) from 20 June–14 August at Gotland Deep. Fe(II), O_2 and H_2O_2 values refer to 5 m water depth.

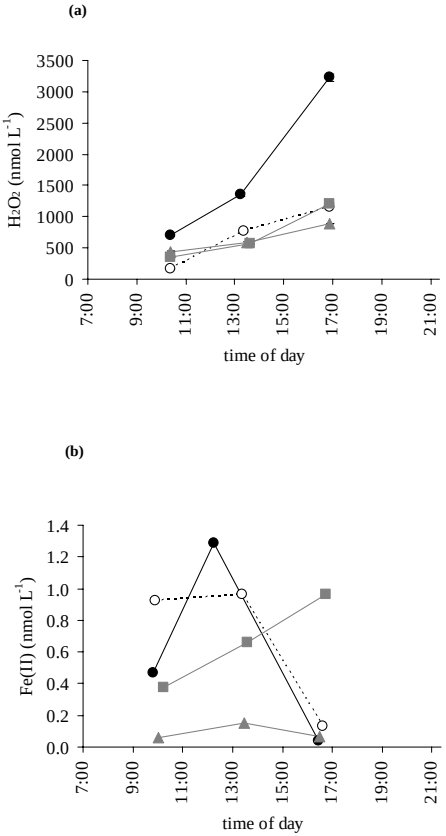

Fig. 11. Deck incubation experiments carried out during 20 July at Gotland Deep. **(a)** Development of hydrogen peroxide (H_2O_2) during the day measured in 0.2 μm filtered seawater (solid black circles), untreated seawater (open circles), seawater depleted of heterocystous cyanobacteria (grey squares), and seawater enriched with heterocystous cyanobacteria (grey triangles). **(b)** Development of Fe(II) during the day. Treatments are depicted as in A.